

# Física do Corpo Humano (4300325)



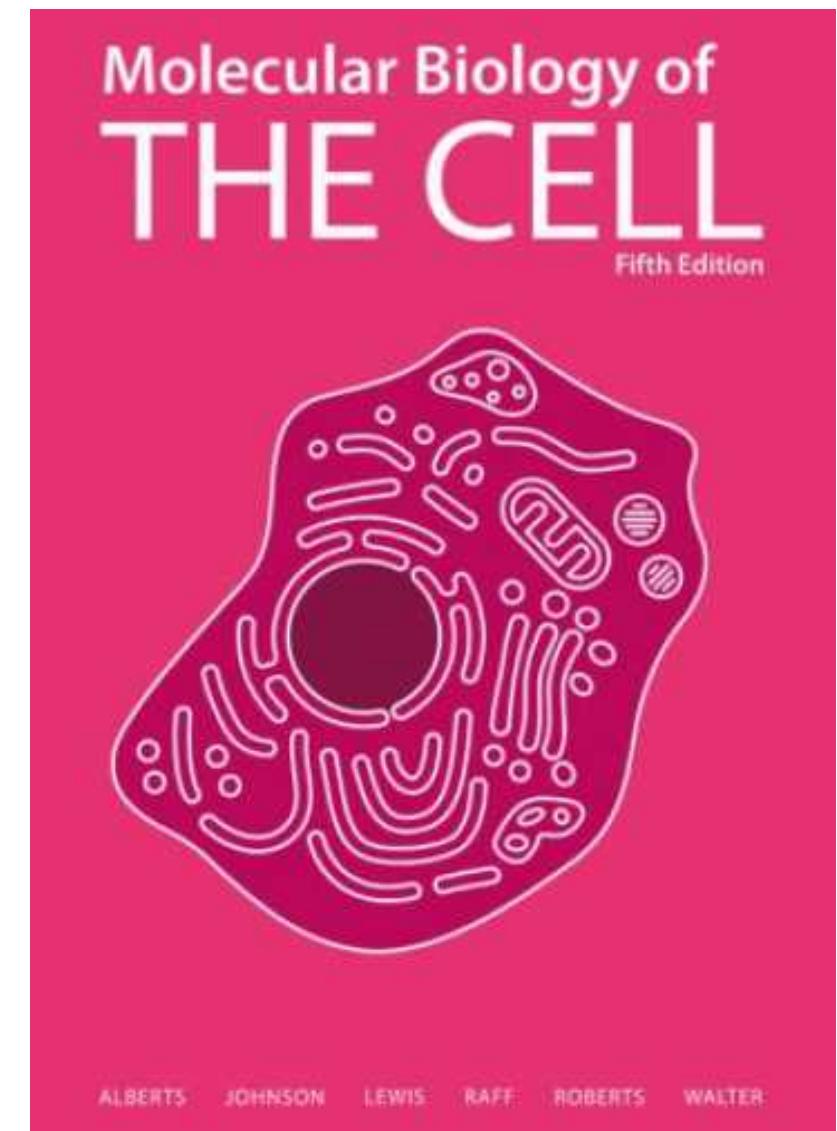
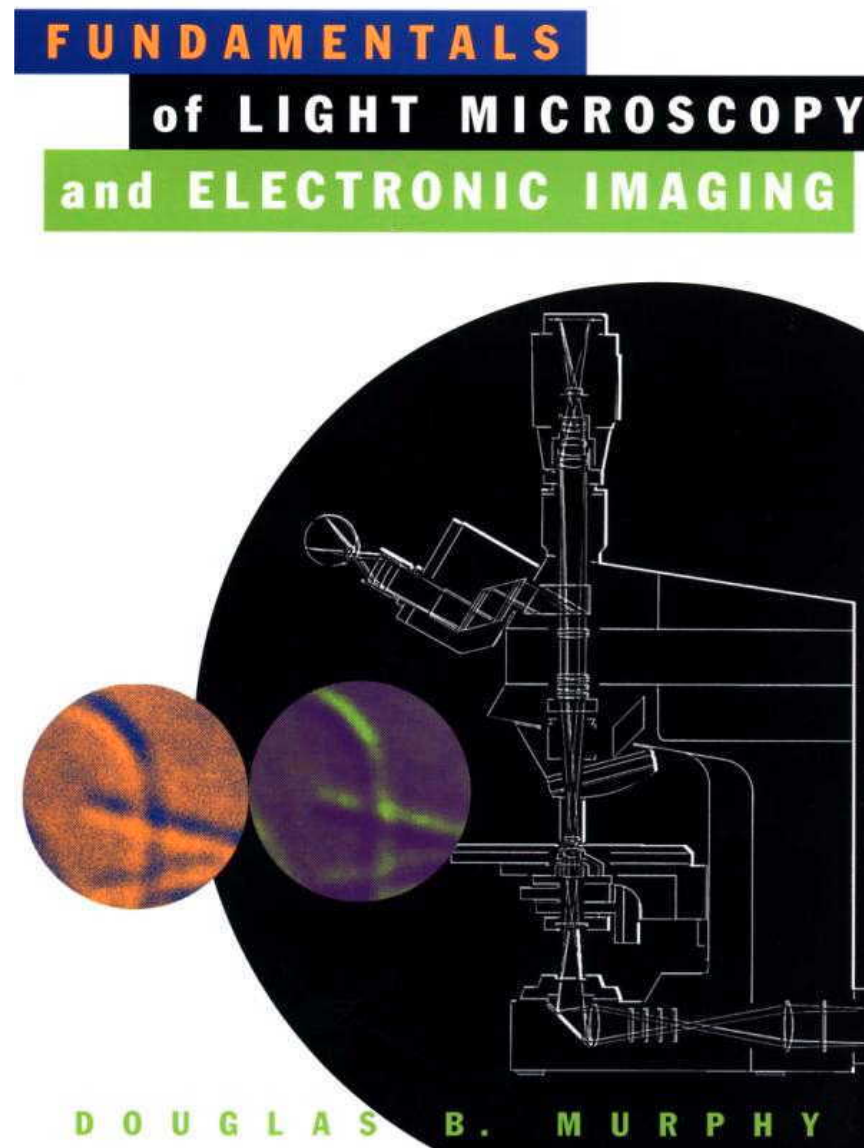
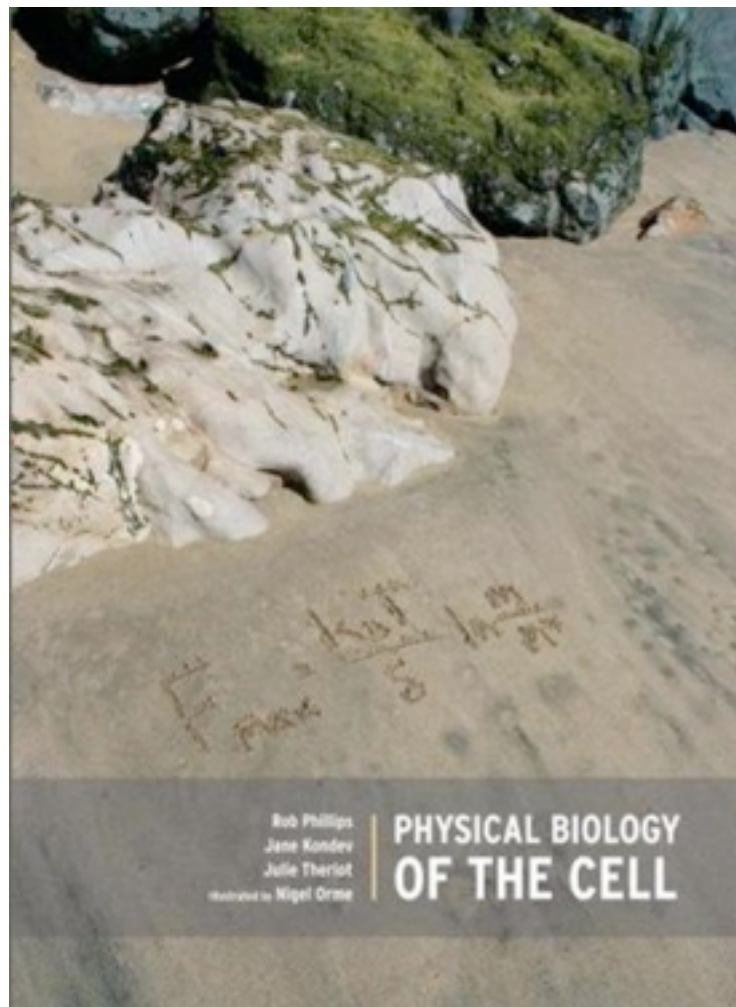
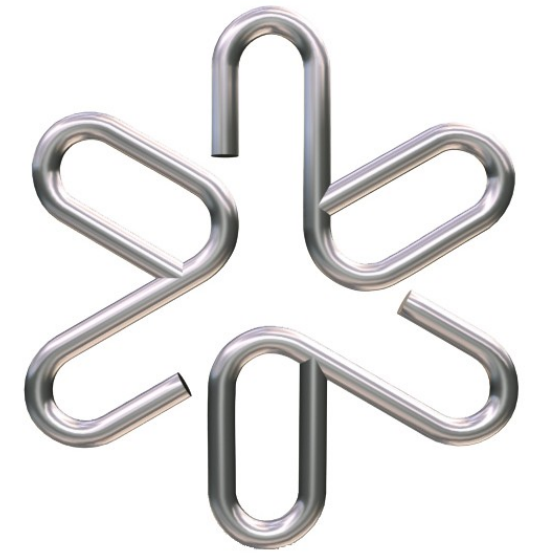
Prof. Adriano Mesquita Alencar  
Dep. Física Geral  
Instituto de Física da USP

**B06**

**Microscopia**  
**Aula 10**



# Fisica do Corpo Humano (4300325)



# Microscópio

**1300** - Lentes para observar coisas pequenas

**1660** - Marcello Malpighi usou lentes compostas (microscopio para ver capilares sangüíneos em rabos de peixes vivos.

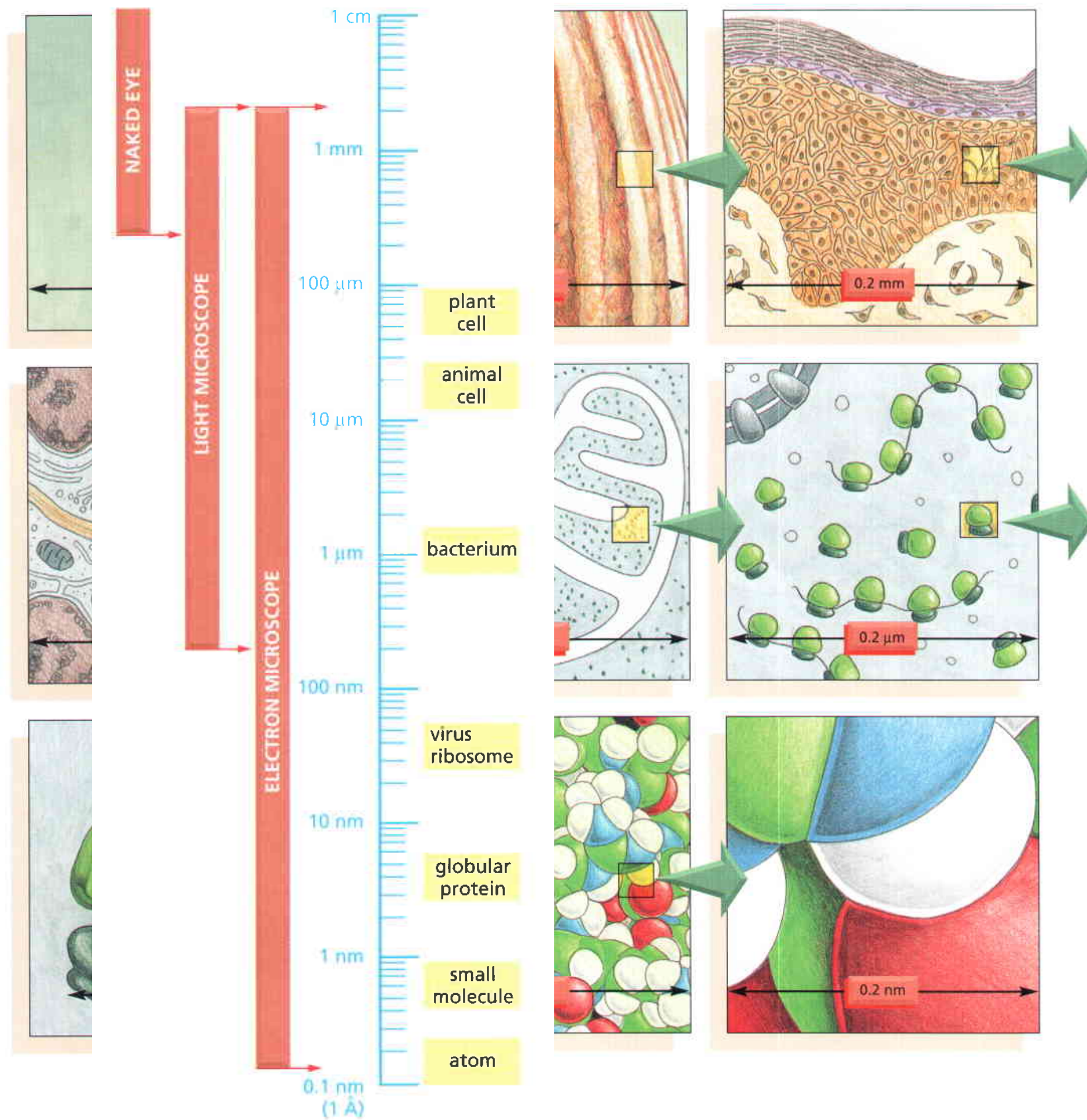
**1665** - Robert Hooke encontrou elementos em cortiça que ele batizou de “células” (na verdade não eram células)

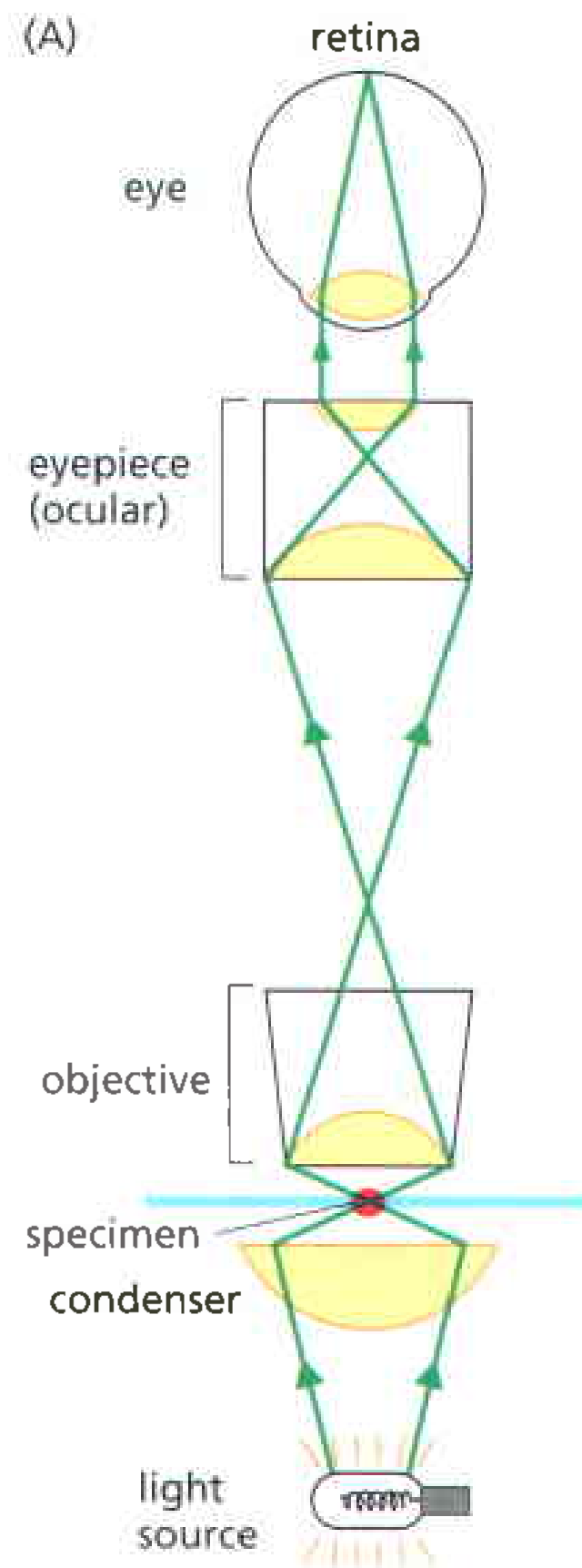
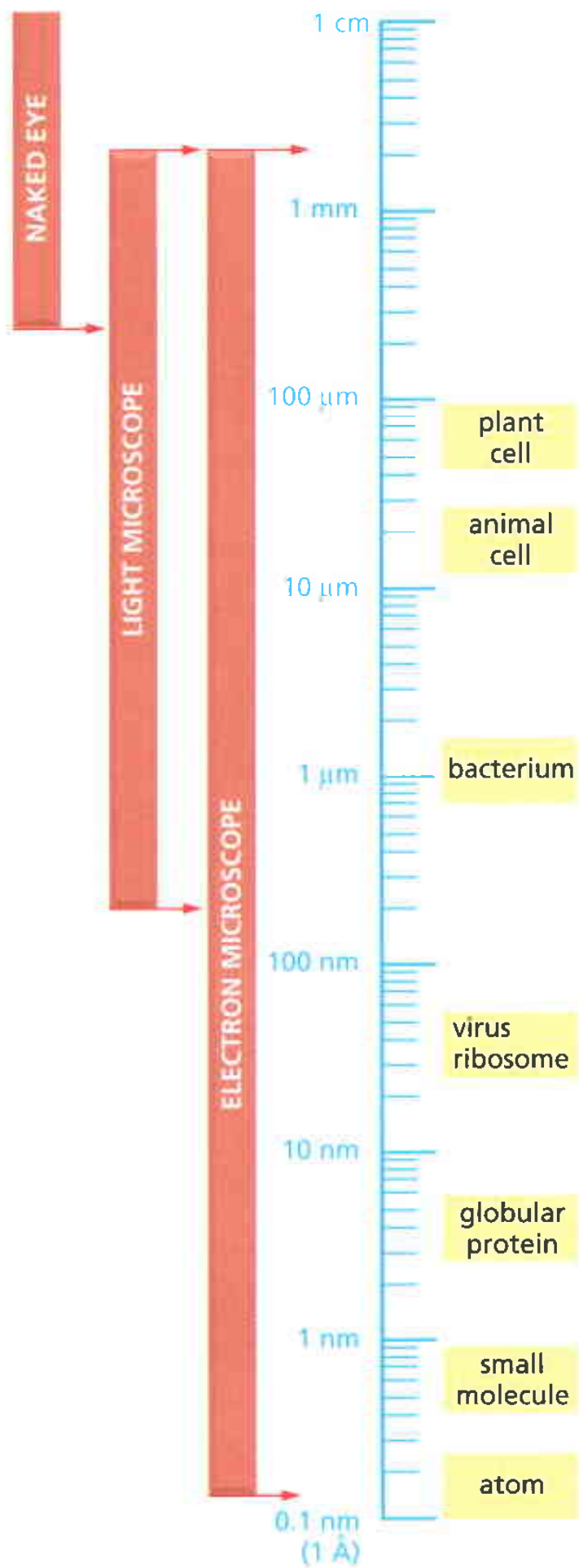
**1838** - Teoria Celular

**1900** - microscopia eletrônica



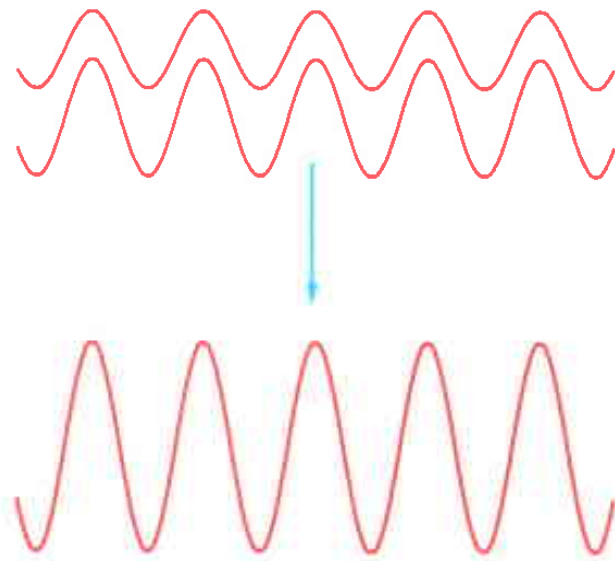
# Microscopia, ordem de grandeza





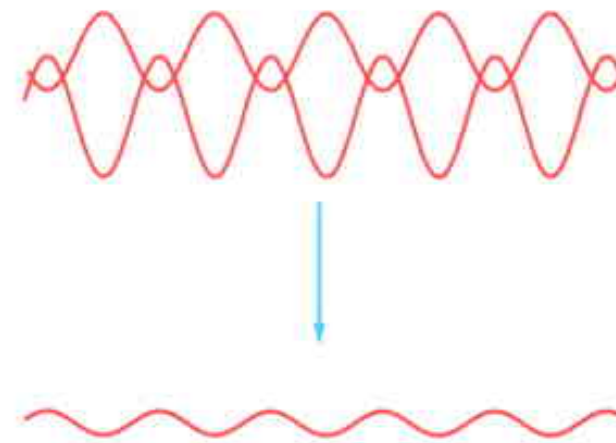
# Interferência Óptica

TWO WAVES IN PHASE

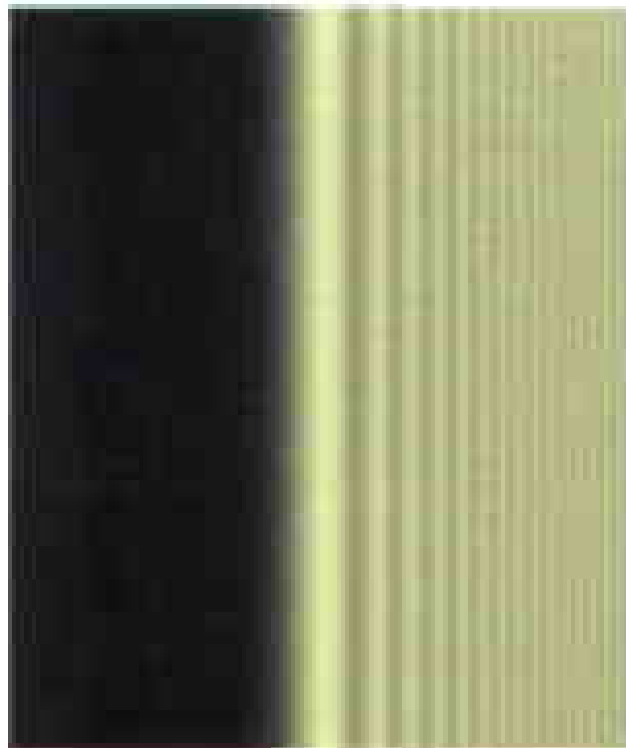


BRIGHT

TWO WAVES OUT OF PHASE



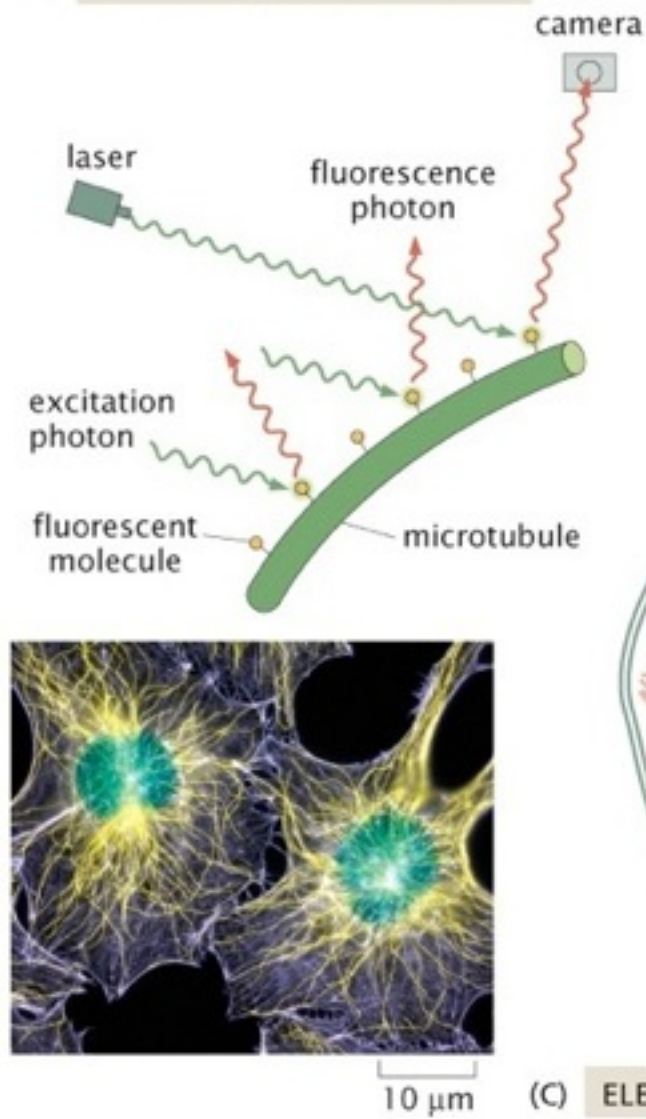
DIM



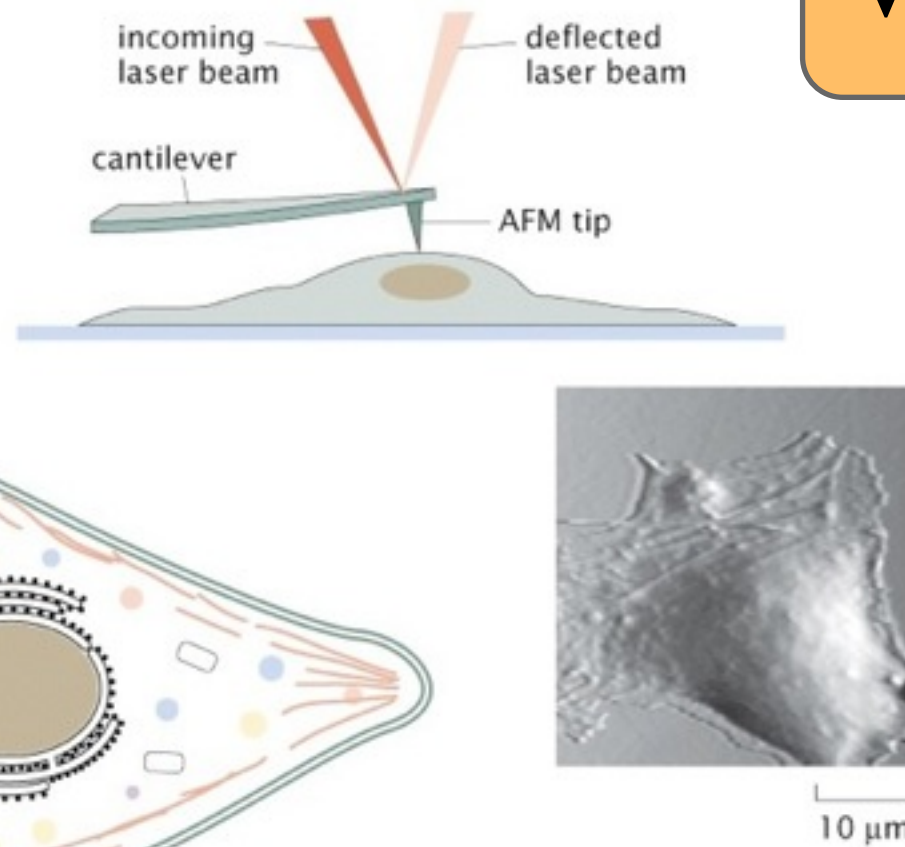


# Visualização

## (A) FLUORESCENCE MICROSCOPY



## (B) ATOMIC-FORCE MICROSCOPY



## (C) ELECTRON MICROSCOPY

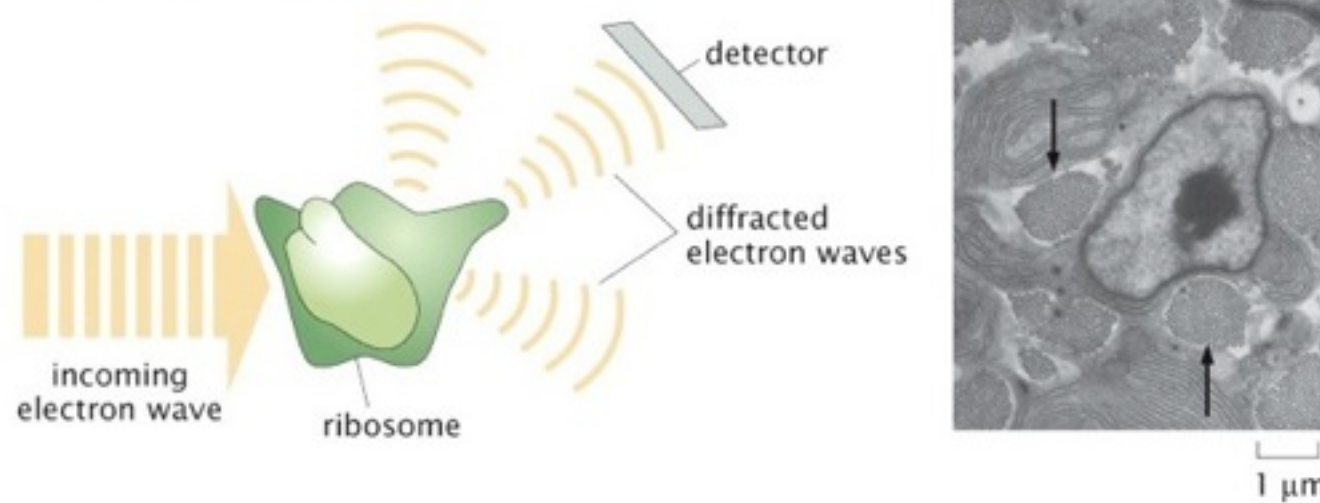


Figure 2.13 Physical Biology of the Cell, 2ed. (© Garland Science 2013)

# Visualização





A resolução de um sistema pode ser limitado por dois fatores de origens diferentes e não correlacionados:

1) aberração (morfológica ou cromática explicada via óptica geométrica). Pode ser solucionado \$\$\$

2) difração (originado devido a natureza ondulatória da luz e determinado pela abertura finita dos elementos ópticos)

A resolução angular de um sistema óptico pode ser estimado pelo critério de Rayleigh [Lord Rayleigh: 12 de Novembro de 1842 - 30 de Junho de 1919]. Dois pontos são considerados minimamente resolvidos quando o máximo principal da difração de uma imagem coincide com o primeiro mínimo de uma outra imagem. Considerando a difração de uma onda  $\lambda$ , por uma abertura circular de diâmetro  $D$ :

$$\sin \theta = 1.220 \frac{\lambda}{D}$$

Onde  $\theta$  é a resolução angular.

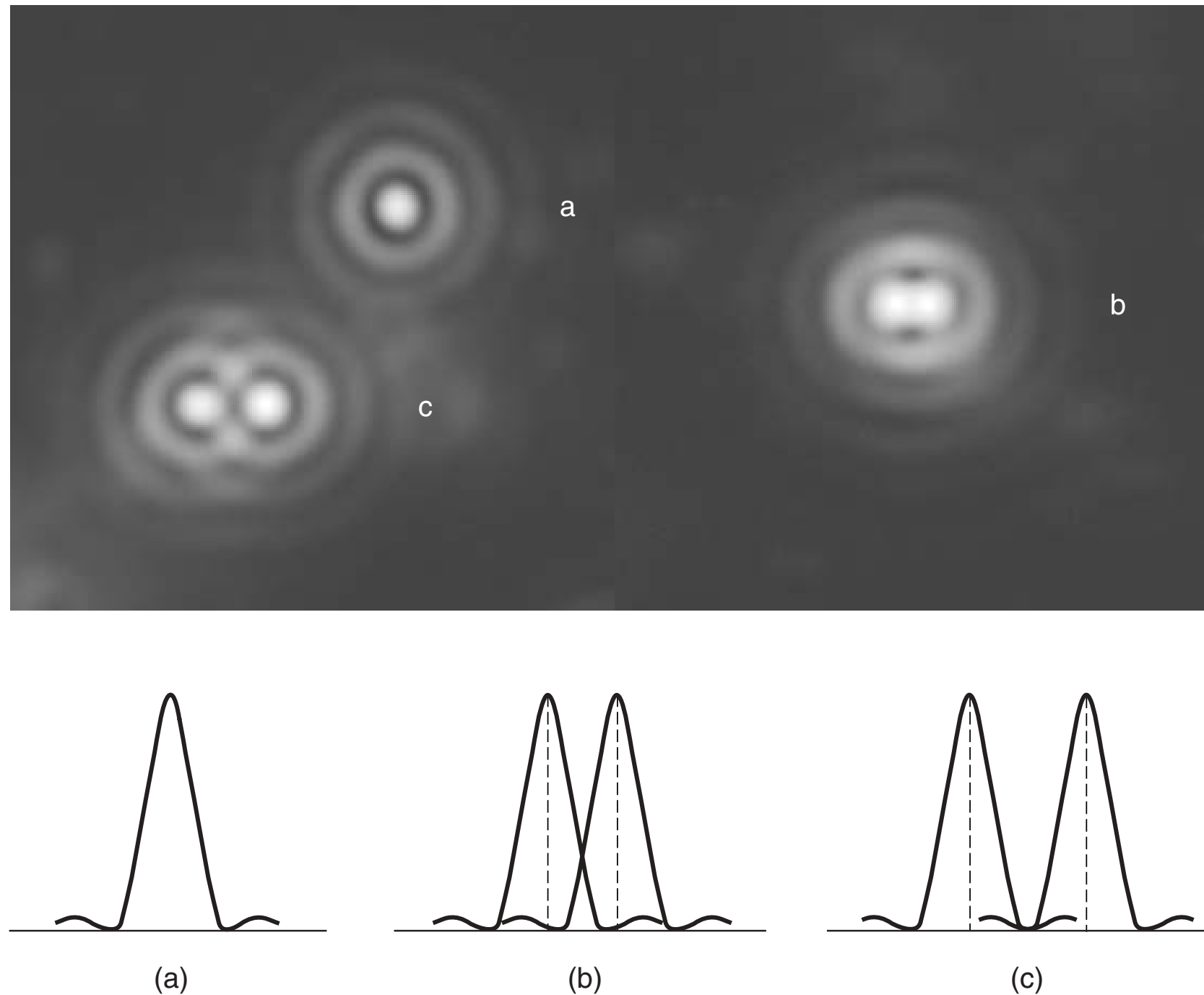
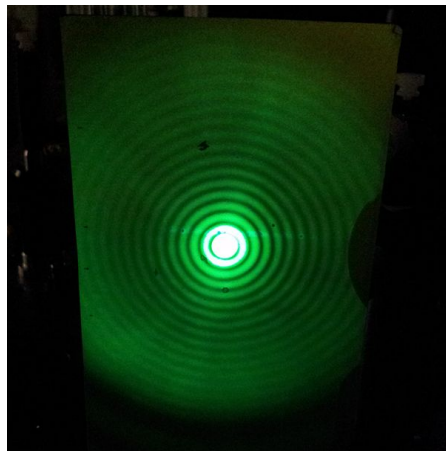


**Figure 6-3**

Rayleigh criterion for spatial resolution. (a) Profile of a single diffraction pattern: The bright Airy disk and 1st- and 2nd-order diffraction rings are visible. (b) Profile of two disks separated at the Rayleigh limit such that the maximum of a disk overlaps the first minimum of the other disk: The points are now just barely resolved. (c) Profile of two disks at a separation distance such that the maximum of each disk overlaps the second minimum of the other disk: The points are clearly resolved.

O fator 1.22 vem de um cálculo da posição do primeiro círculo escuro em torno de um disco de Airy (1.22 é aproximadamente o primeiro zero da Função de Bessel de primeiro tipo, de ordem 1, ( $J_1$ ) dividido por  $\pi$ ).



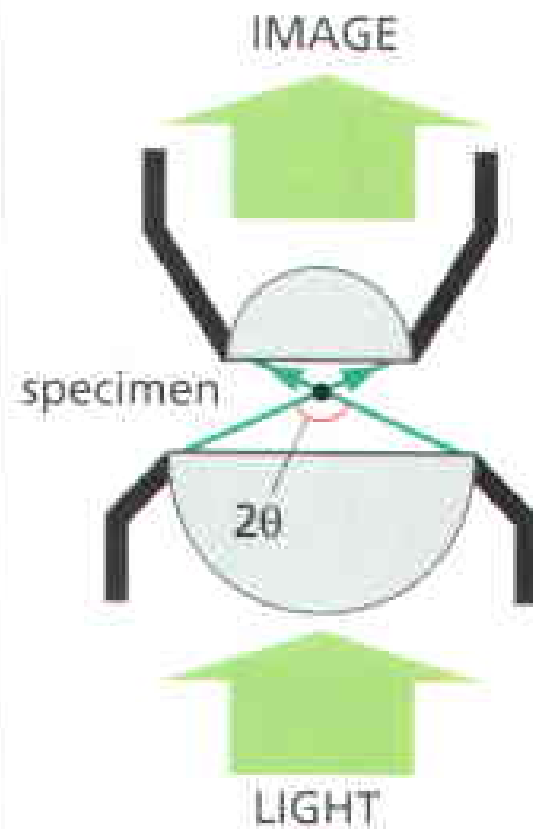
A resolução de um microscópio é medida em distância:

$$R = 1.220 \frac{\lambda}{NA_{\text{condensador}} + NA_{\text{objetiva}}}, \quad \text{onde } NA = n \sin \theta$$

$NA$  é a abertura numérica, e  $n$  o índice de refração entre a amostra e a lente. Se as duas  $NAs$  forem iguais  $R = 0.61 \lambda / NA$



## LENSES



the **objective** lens collects a cone of light rays to create an image

the **condenser** lens focuses a cone of light rays onto each point of the specimen

**RESOLUTION:** the resolving power of the microscope depends on the width of the cone of illumination and therefore on both the condenser and the objective lens. It is calculated using the formula

$$\text{resolution} = \frac{0.61 \lambda}{n \sin \theta}$$

where:

$\theta$  = half the angular width of the cone of rays collected by the objective lens from a typical point in the specimen (since the maximum width is  $180^\circ$ ,  $\sin \theta$  has a maximum value of 1)

$n$  = the refractive index of the medium (usually air or oil) separating the specimen from the objective and condenser lenses

$\lambda$  = the wavelength of light used (for white light a figure of  $0.53 \mu\text{m}$  is commonly assumed)

**NUMERICAL APERTURE:**  $n \sin \theta$  in the equation above is called the numerical aperture of the lens (NA) and is a function of its light-collecting ability. For dry lenses this cannot be more than 1, but for oil-immersion lenses it can be as high as 1.4. The higher the numerical

aperture, the greater the resolution and the brighter the image (brightness is important in fluorescence microscopy). However, this advantage is obtained at the expense of very short working distances and a very small depth of field.

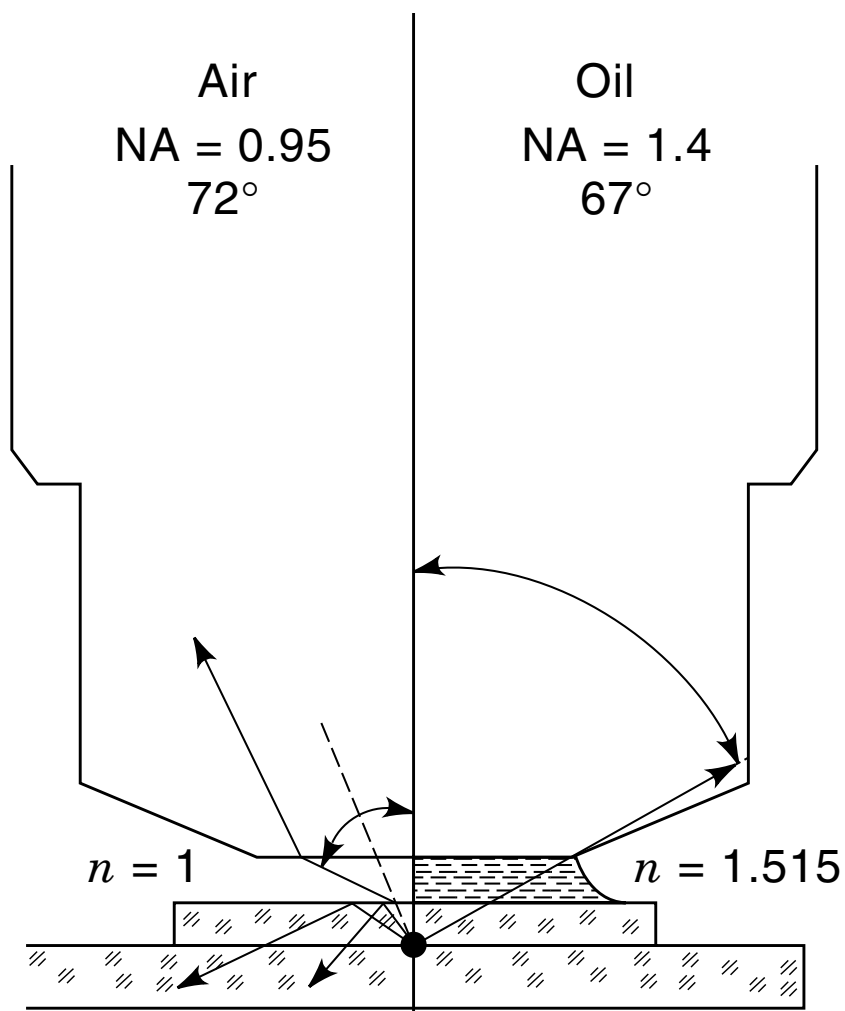


**Figure 6-2**

Effect of immersion oil on increasing the angular extent over which diffracted rays can be accepted by an objective lens. Numerical aperture is directly dependent on the wavelength  $\lambda$  and the sine of the half angle of the cone of illumination  $\theta$  accepted by the front lens of the objective. For dry lenses, NA is limited, because rays subtending angles of  $41^\circ$  or greater are lost by total internal reflection and never enter the lens (dotted line). The practical limit for a dry lens is  $\sim 39^\circ$ , which corresponds to an acceptance angle of  $72^\circ$ , and an NA of 0.95. By adding high-refractive index immersion oil matching that of the glass coverslip ( $n = 1.515$ ), an oil immersion objective can collect light diffracted up to  $67^\circ$ , which corresponds to NA = 1.4.

# Interferência Óptica

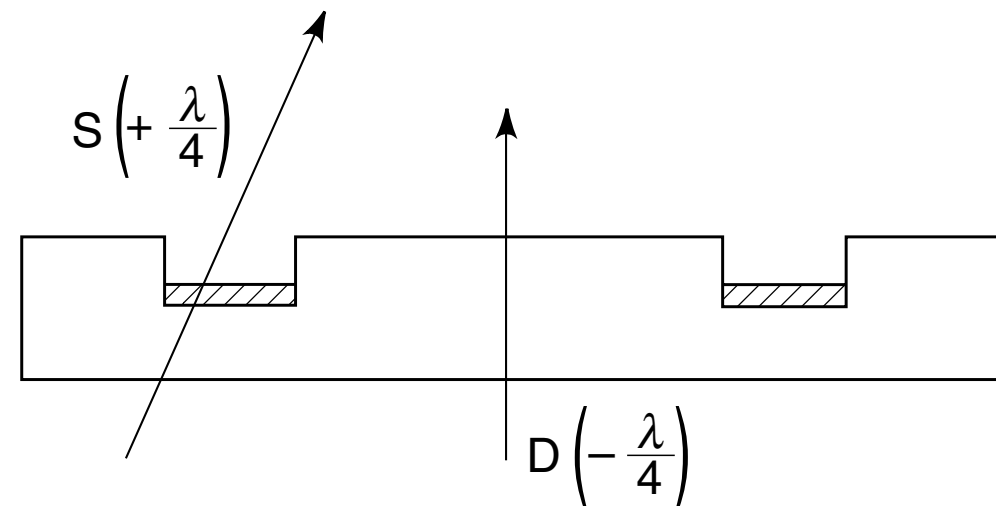
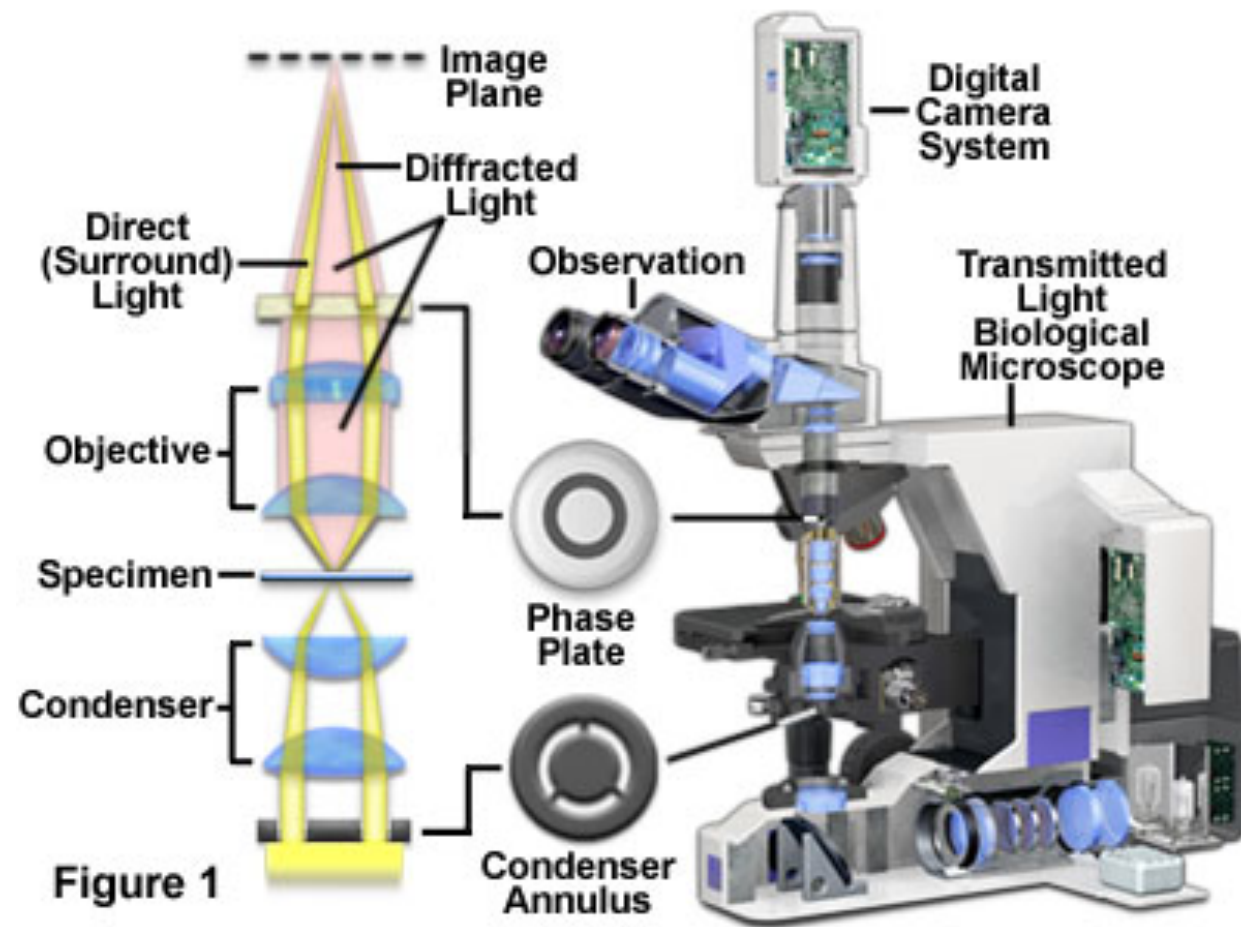


Figure 7-7

The action of a phase plate at the rear surface of the objective lens. Surround or background rays (S) are advanced in phase relative to the D wave by  $\lambda/4$  at the phase plate. Relative phase advancement is created by etching a ring in the plate that reduces the physical path taken by the S waves through the high-refractive-index plate. Since diffracted object rays (D) are retarded by  $\lambda/4$  at the specimen, the optical path difference between D and S waves upon emergence from the phase plate is  $\lambda/2$ , allowing destructive interference in the image plane. The recessed ring in the phase plate is made semitransparent so that the amplitude of the S wave is reduced by 70–75% to optimize contrast in the image plane.



## Phase Contrast Microscope Configuration



## Phase Contrast Microscope Optical Train

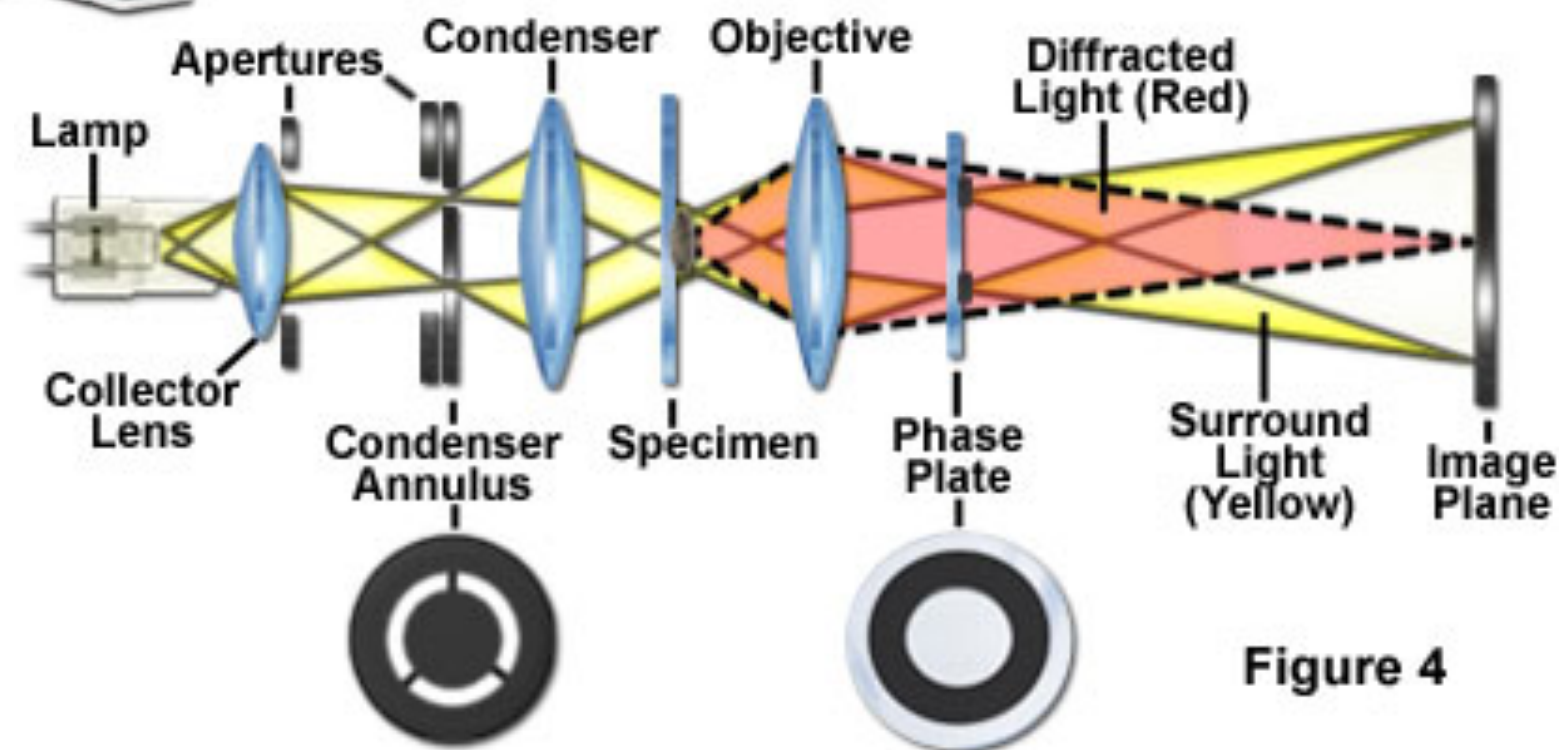


Figure 4

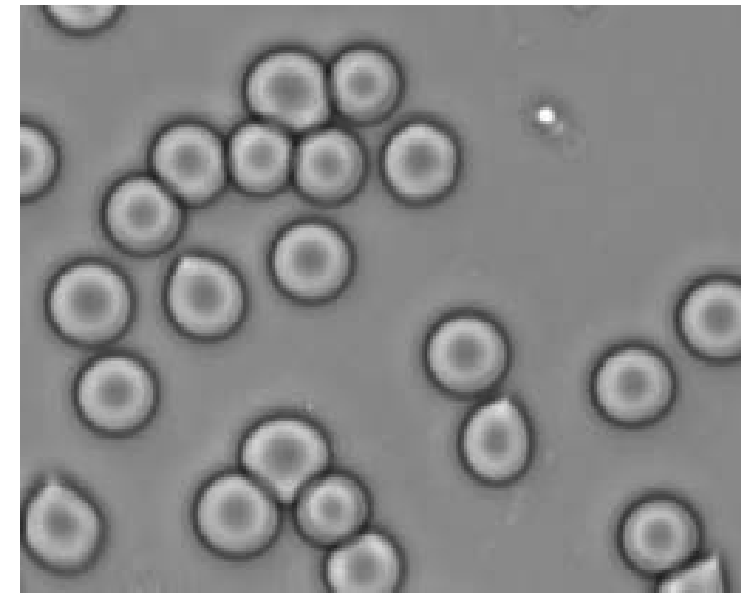
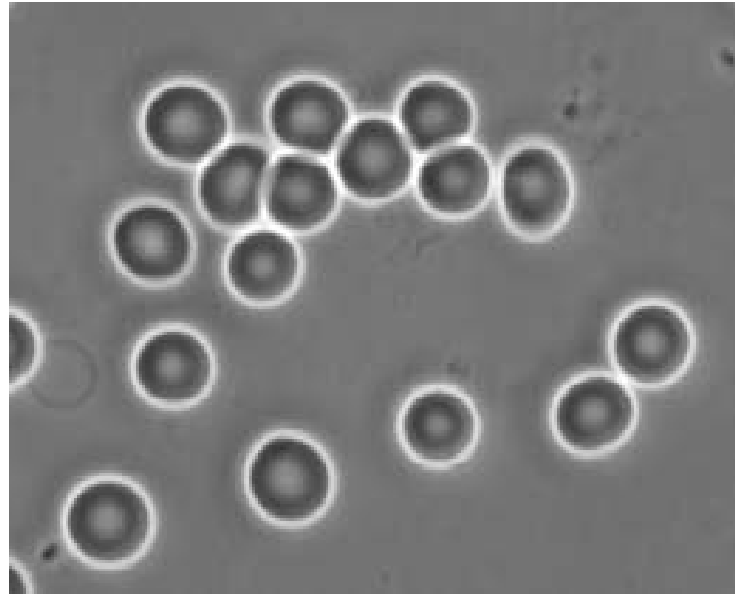
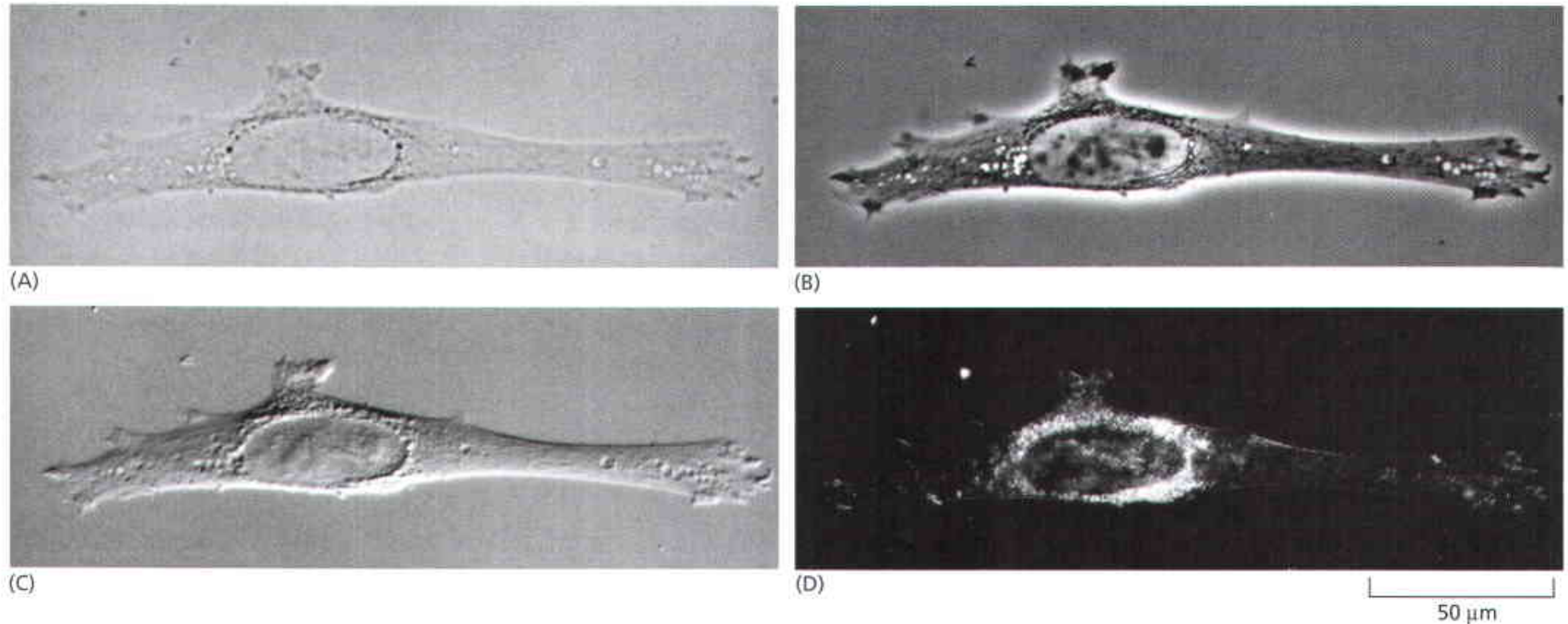


Figure 7-8

Comparison of positive and negative phase contrast systems. Shown in pairs, from the top down: phase plates for advancing (positive contrast) or retarding (negative contrast) the surround wave; amplitude profiles of waves showing destructive interference (positive phase contrast) and constructive interference (negative phase contrast) for a high-refractive-index object. Notice that the phase plate advances or retards the S wave relative to the D wave. The amplitude of the resultant P wave is lower or higher than the S wave, causing the object to look relatively darker or brighter than the background. Vector diagrams showing advancement of the S wave by  $\lambda/4$ , which is shown as a  $90^\circ$  counterclockwise rotation in positive phase contrast, and retardation of the S wave by  $\lambda/4$ , which is shown as a  $90^\circ$  clockwise rotation in negative phase contrast. Addition of the S and D wave vectors gives P waves whose amplitudes vary relative to the S waves. Images of erythrocytes in positive and negative phase contrast optics.

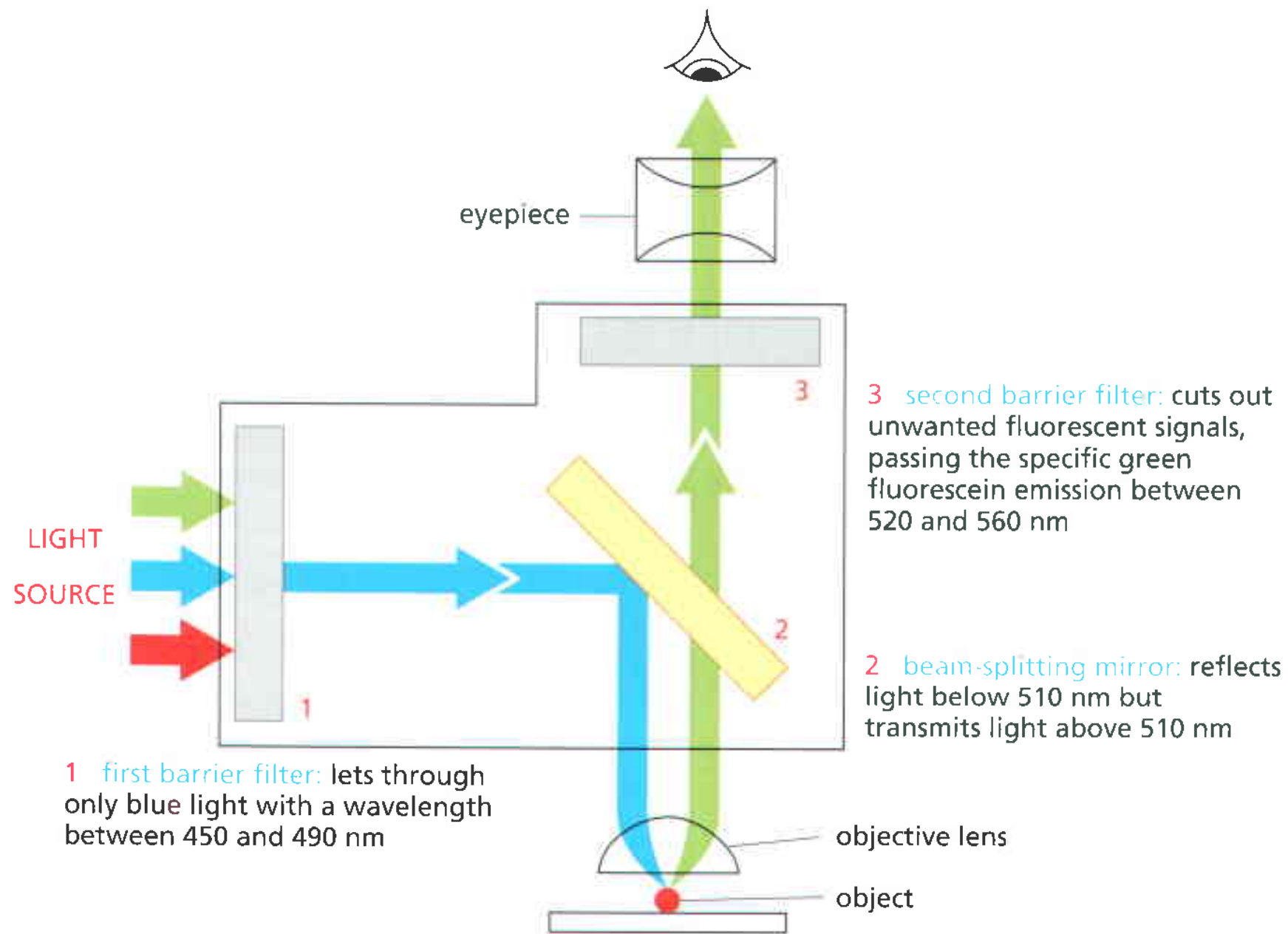
# Interferência Óptica



**Figure 9–8 Four types of light microscopy.** Four images are shown of the same fibroblast cell in culture. All images can be obtained with most modern microscopes by interchanging optical components. (A) Bright-field microscopy. (B) Phase-contrast microscopy. (C) Nomarski differential-interference-contrast microscopy. (D) Dark-field microscopy.



# Microscópio de Fluorescência



# Microscópio de Fluorescência

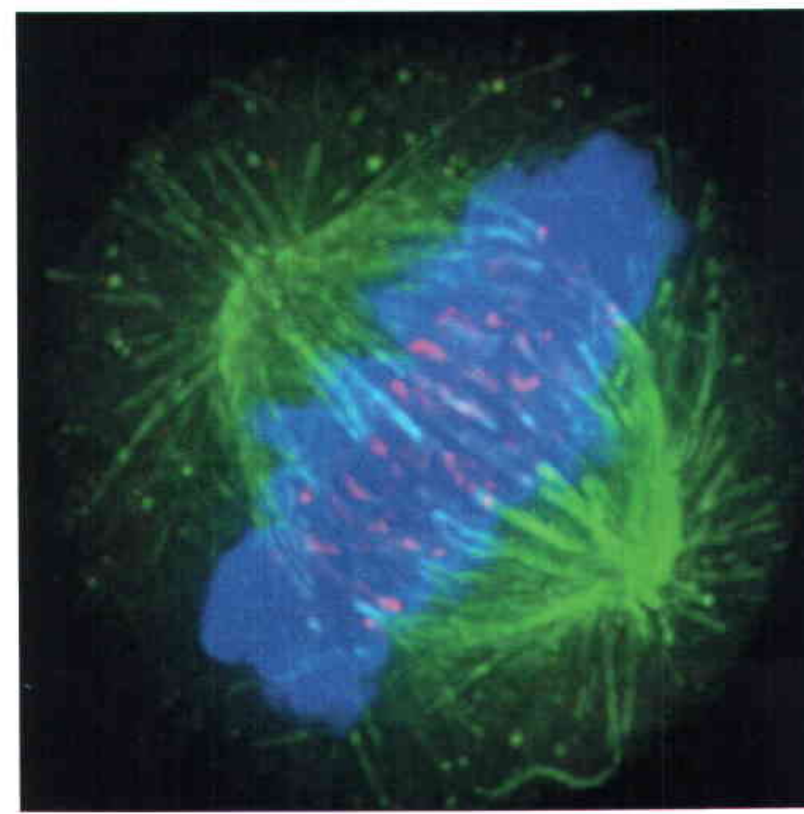
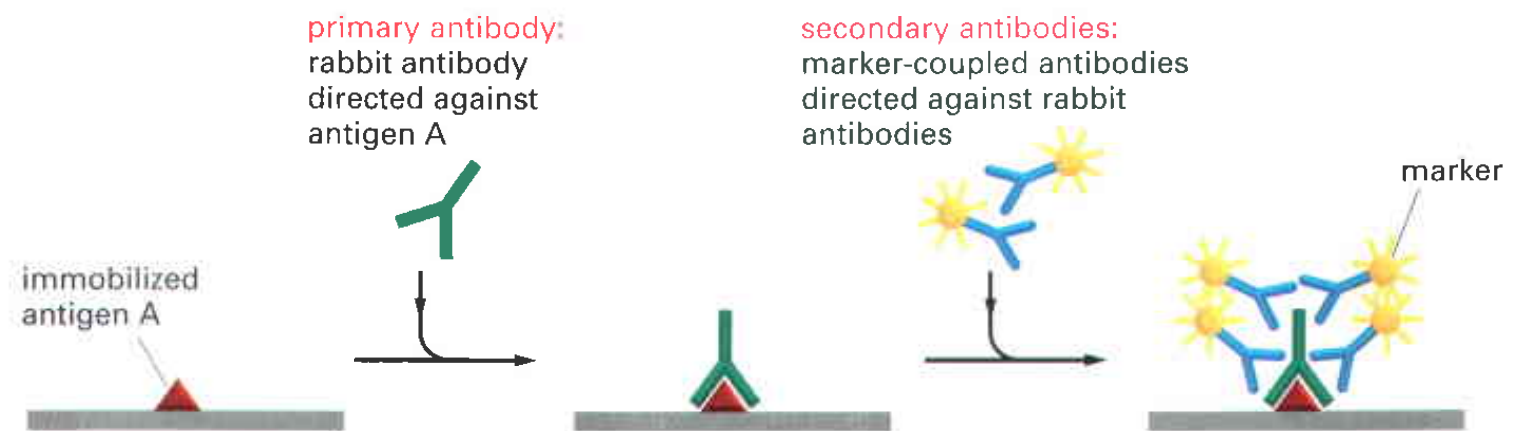
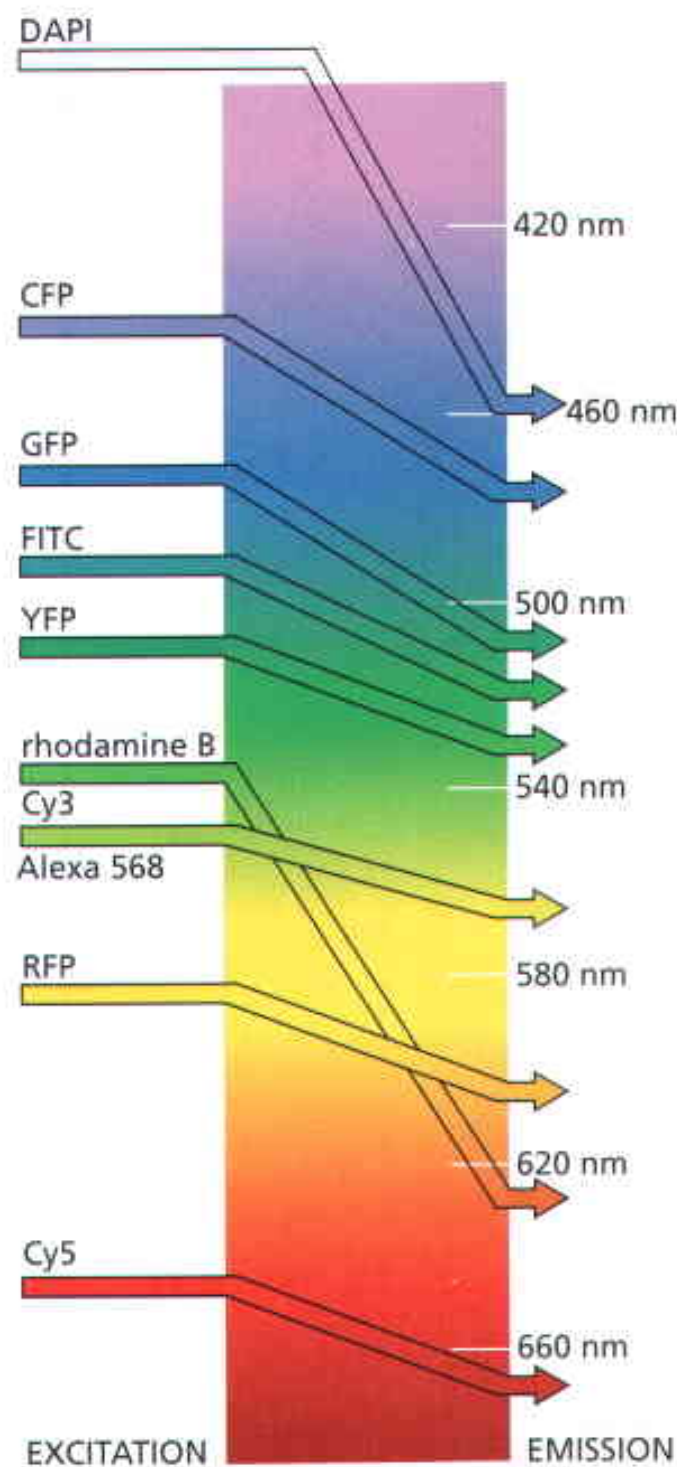


**Figure 9-15 Multiple-fluorescent-probe microscopy.** In this composite micrograph of a cell in mitosis, three different fluorescent probes have been used to stain three different cellular components. <GTCT> The spindle microtubules are revealed with a *green* fluorescent antibody, centromeres with a *red* fluorescent antibody and the DNA of the condensed chromosomes with the *blue* fluorescent dye DAPI. (Courtesy of Kevin F. Sullivan.)

# Microscópio de Fluorescência

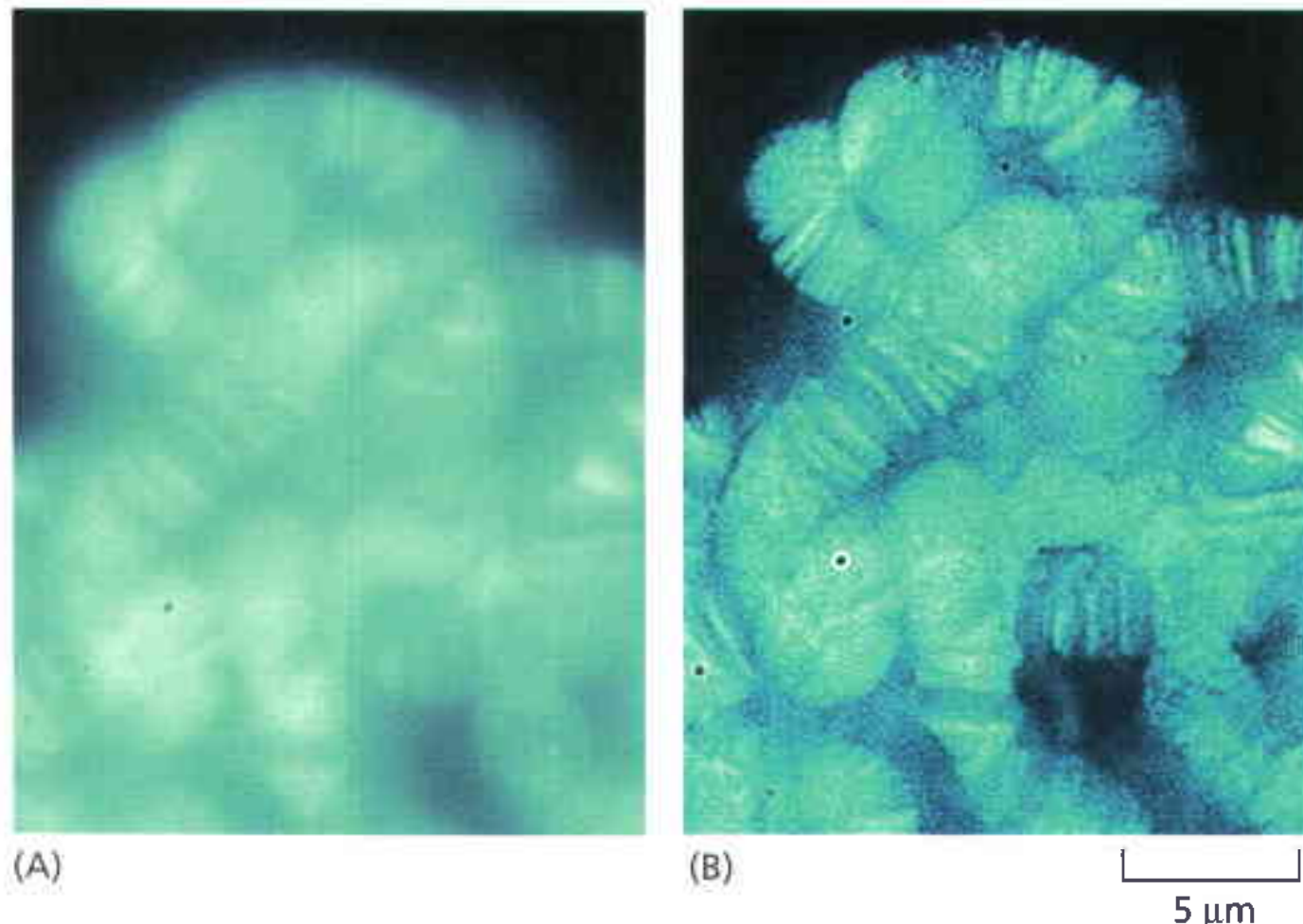
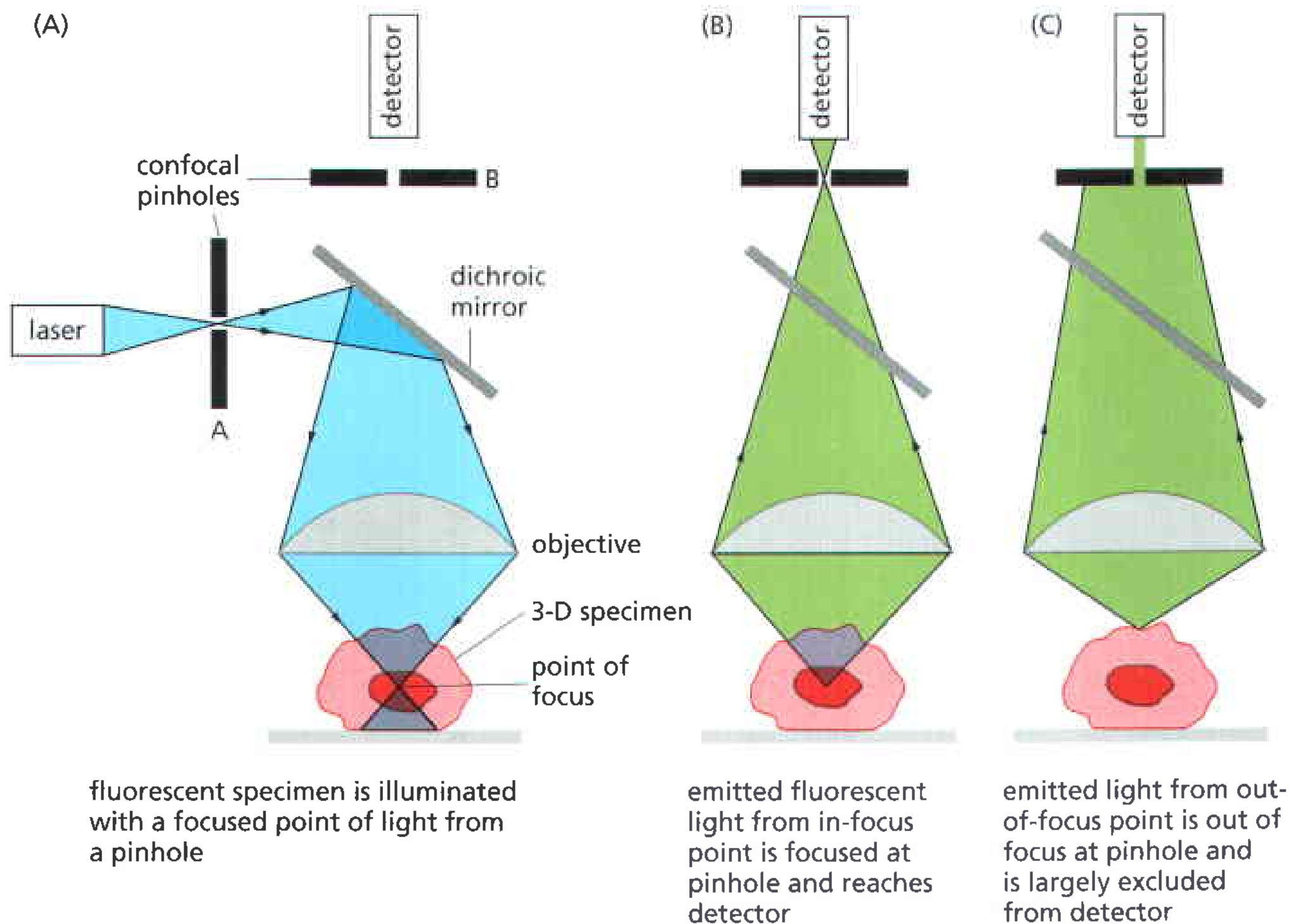


**Figure 9-19 Image deconvolution.**

(A) A light micrograph of the large polytene chromosomes from *Drosophila* stained with a fluorescent DNA-binding dye. (B) The same field of view after image deconvolution clearly reveals the banding pattern on the chromosomes. Each band is about 0.25  $\mu\text{m}$  thick, approaching the resolution limit of the light microscope. (Courtesy of the John Sedat Laboratory.)



# Microscópio de Confocal



# Microscópio de Confocal

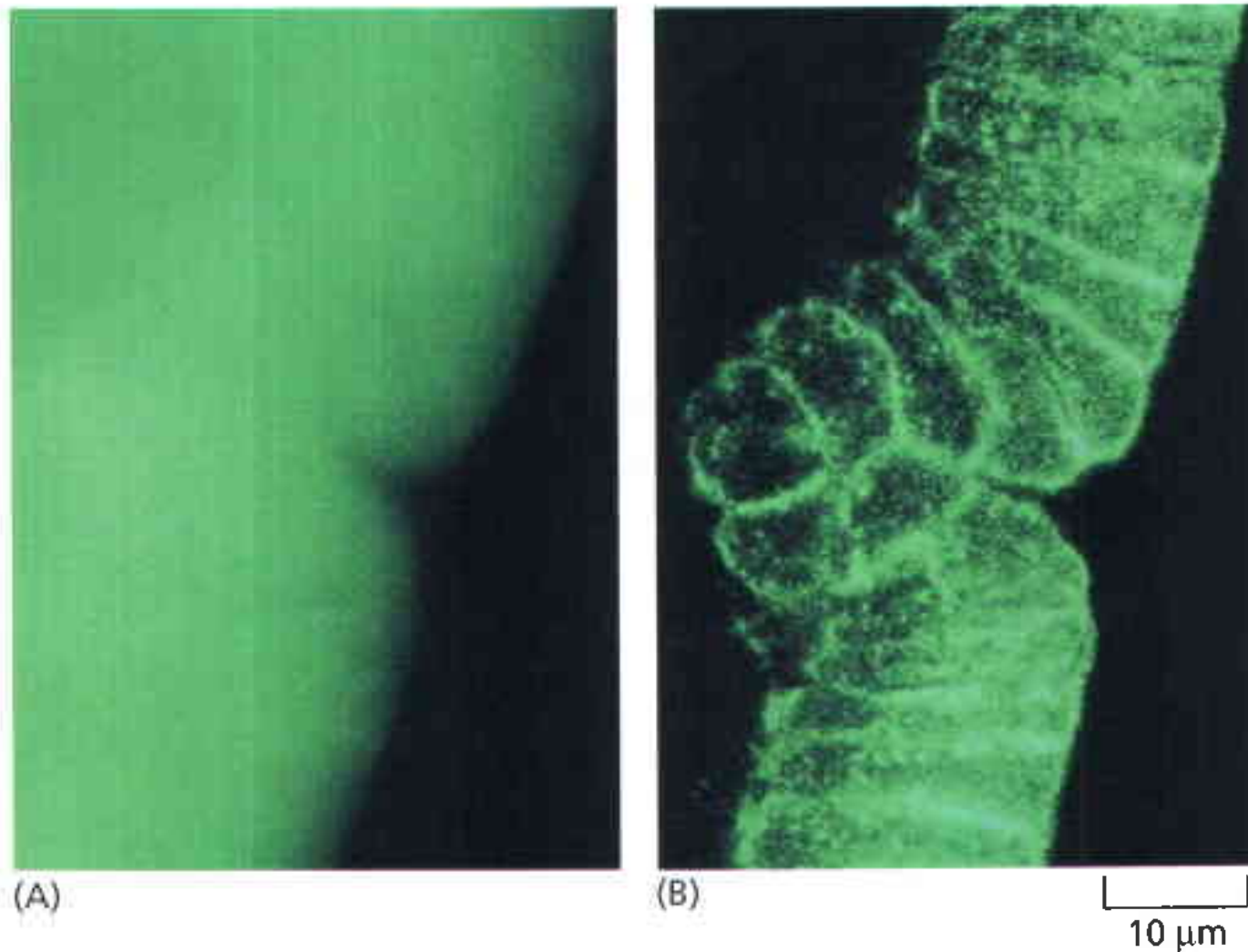
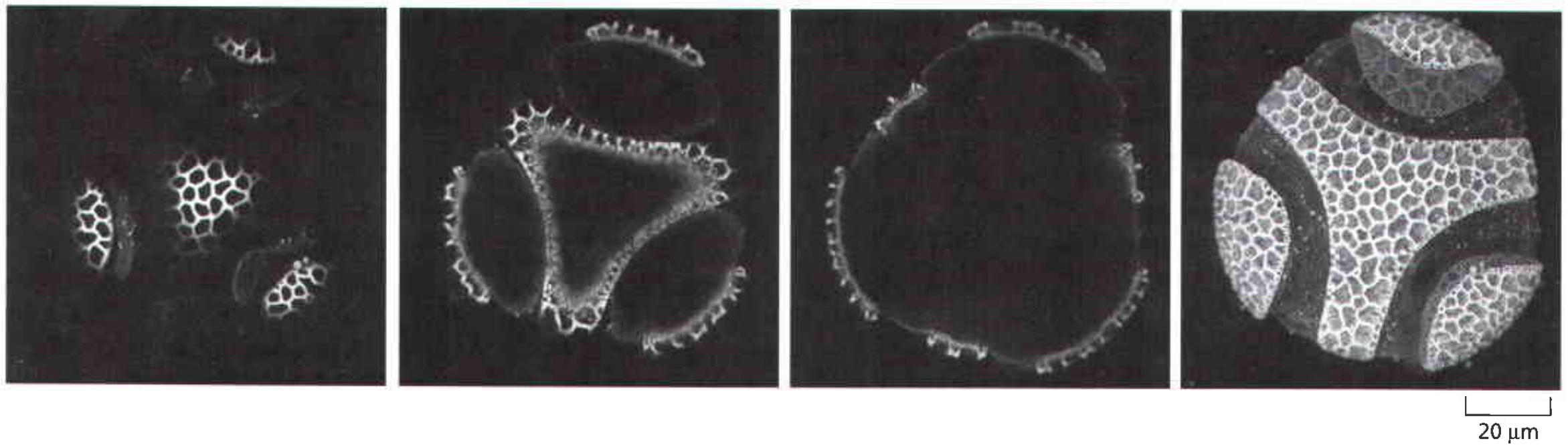


**Figure 9–21 Conventional and confocal fluorescence microscopy compared.** These two micrographs are of the same intact gastrula-stage *Drosophila* embryo that has been stained with a fluorescent probe for actin filaments. (A) The conventional, unprocessed image is blurred by the presence of fluorescent structures above and below the plane of focus. (B) In the confocal image, this out-of-focus information is removed, resulting in a crisp optical section of the cells in the embryo. (Courtesy of Richard Warn and Peter Shaw.)

# Microscópio de Confocal





# Microscópio Eletrônico

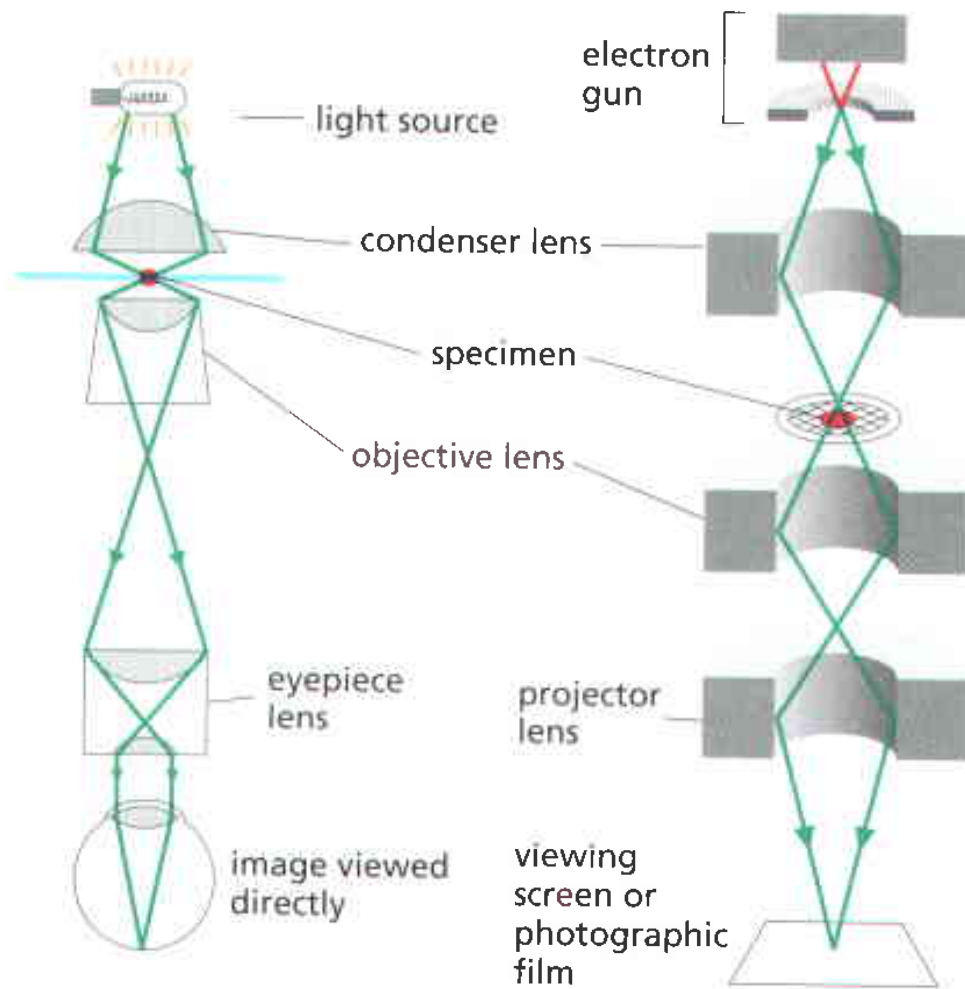


**Figure 9-42** The principal features of a light microscope and a transmission electron microscope. These drawings emphasize the similarities of overall design. Whereas the lenses in the light microscope are made of glass, those in the electron microscope are magnetic coils. The electron microscope requires that the specimen be placed in a vacuum. The inset shows a transmission electron microscope in use. (Photograph courtesy of FEI Company Ltd.)

# Microscópio Eletrônico

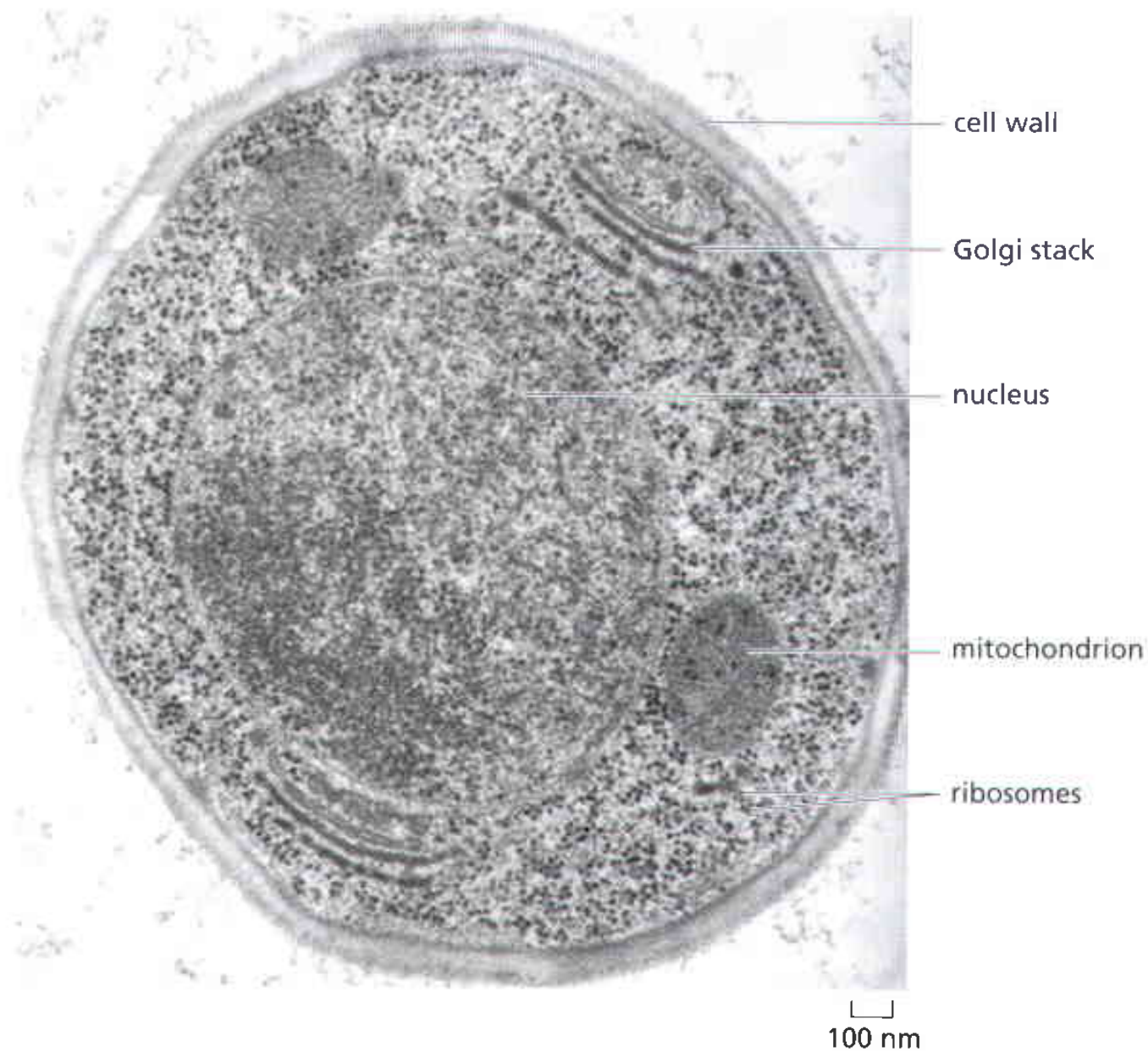


**Figure 9–45 Thin section of a cell.** This thin section is of a yeast cell that has been very rapidly frozen and the vitreous ice replaced by organic solvents and then by plastic resin. The nucleus, mitochondria, cell wall, Golgi stacks, and ribosomes can all be readily seen in a state that is presumed to be as life-like as possible. (Courtesy of Andrew Staehelin.)

# Microscópio Eletrônico

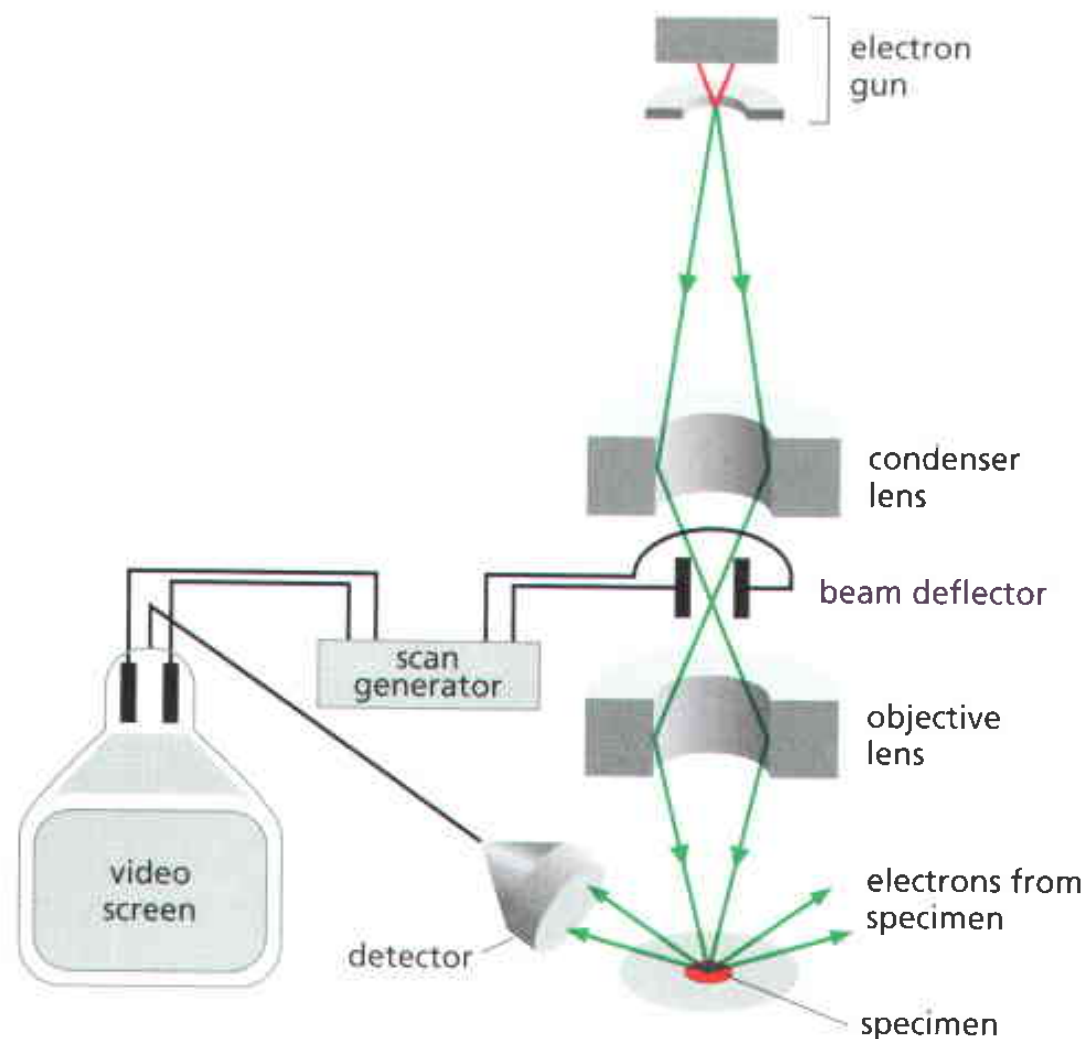
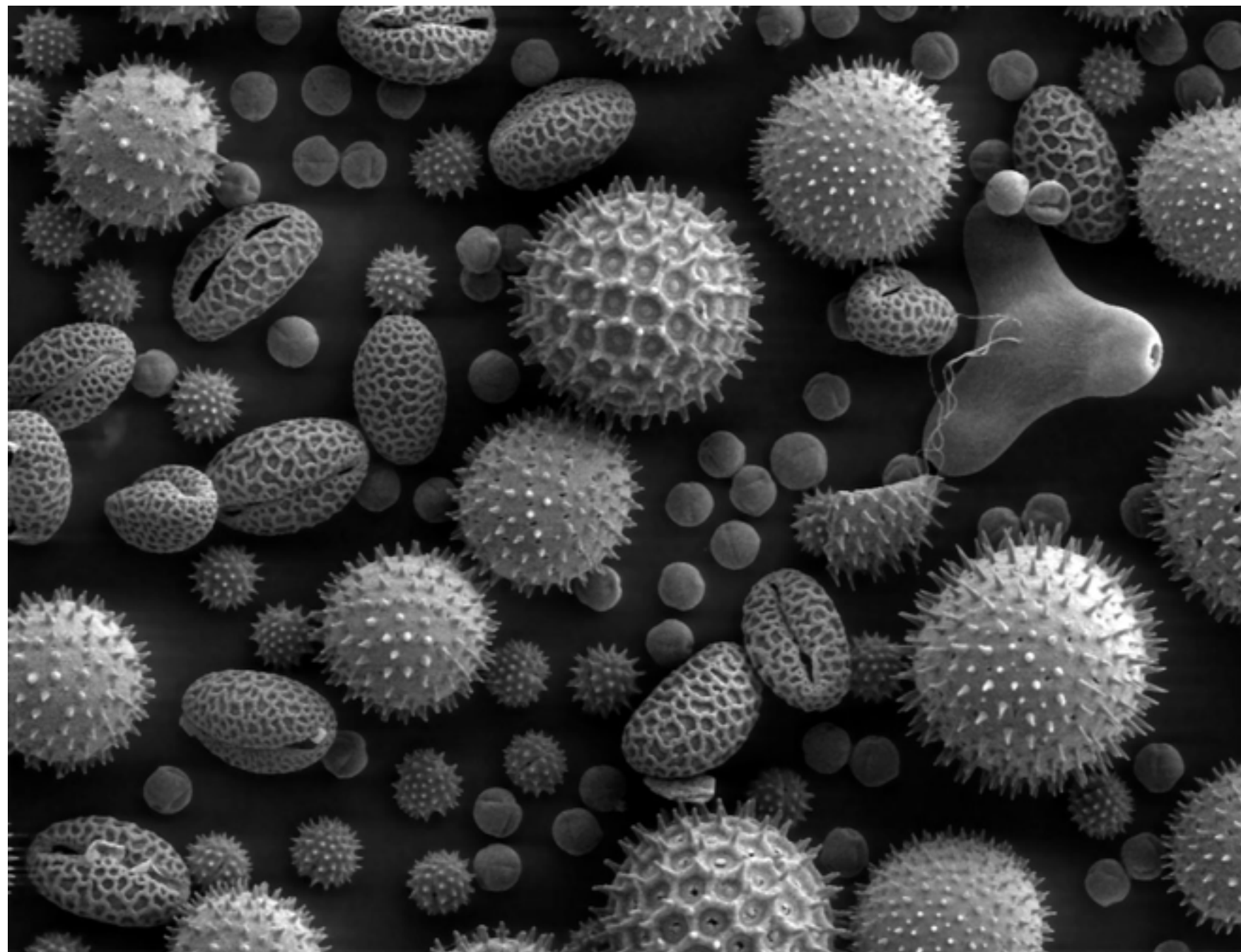


**Figure 9-49 The scanning electron microscope.** In a SEM, the specimen is scanned by a beam of electrons brought to a focus on the specimen by the electromagnetic coils that act as lenses. The detector measures the quantity of electrons scattered or emitted as the beam bombards each successive point on the surface of the specimen and controls the intensity of successive points in an image built up on a video screen. The SEM creates striking images of three-dimensional objects with great depth of focus and a resolution between 3 nm and 20 nm depending on the instrument. (Photograph courtesy of Andrew Davies.)

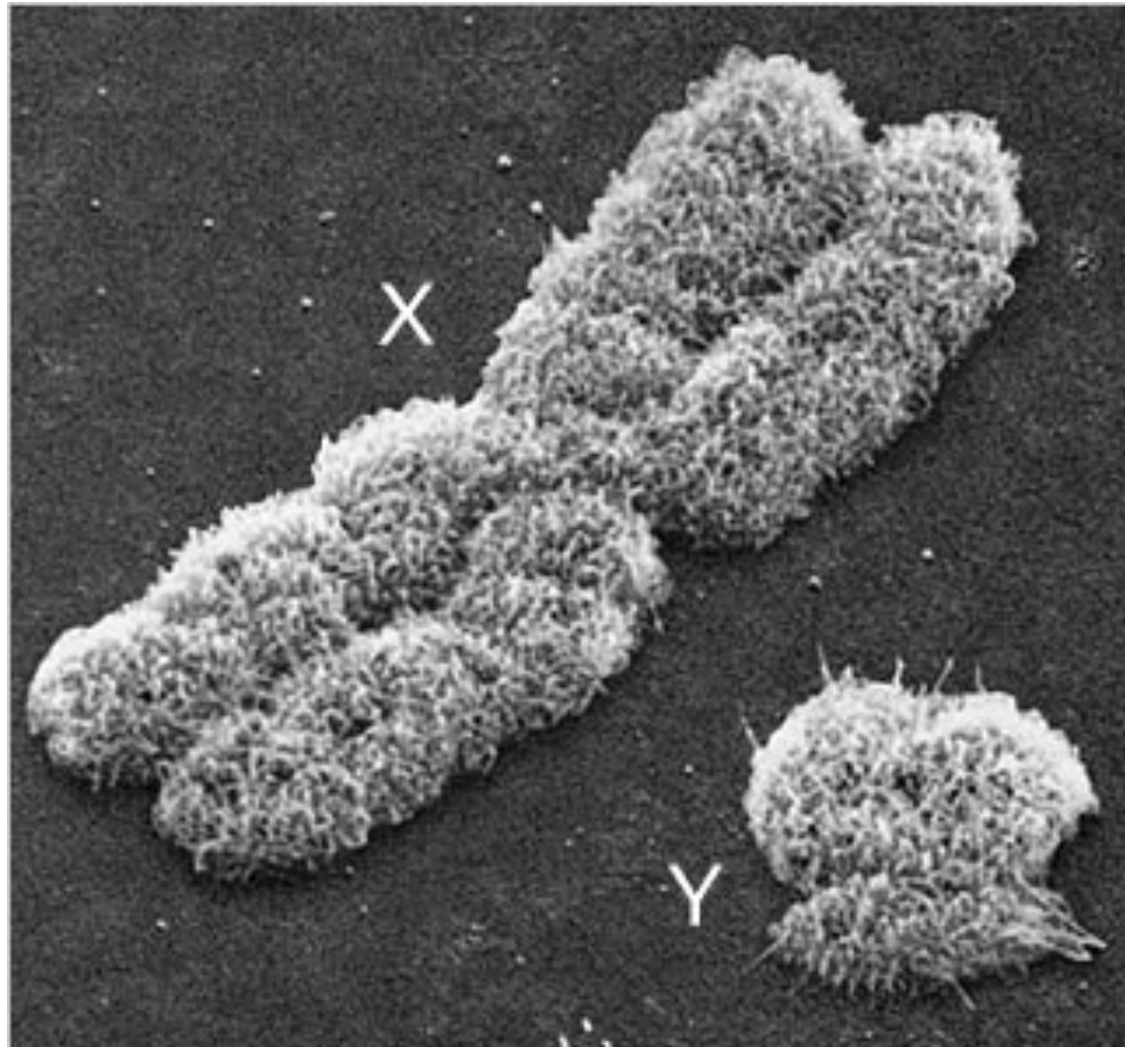


# Microscópio Eletrônico



Grão de  
Pólen

# Microscópio Eletrônico



Cromossomos

# Microscópio Eletrônico



schistosome  
parasite